Physical Review & Research International
3(3): 161-175, 2013

SCIENCEDOMAIN *international*
www.sciencedomain.org

Method for Constraining Light Speed Anisotropy by Using Fiber Optics Gyroscope Experiments

A. Sfarti[1*]

[1]*UC Berkeley, CS Dept, 387 Soda Hall, Berkeley, CA 94720, USA.*

Author's contribution

This work was carried by the author. Author AS designed the study, performed the experiment and the statistical analysis, wrote the protocol, and wrote the first draft of the manuscript. The author read and approved the final manuscript.

Research Article

Received 6th February 2013
Accepted 23rd March 2013
Published 2nd April 2013

ABSTRACT

The Mansouri-Sexl theory is a well known test theory of relativity. Mansouri and Sexl dealt with the theory of the Michelson-Morley, Kennedy-Thorndike and Ives-Stilwell experiments but left out the very interesting Sagnac experiment. In the following paper we will present a novel way of detecting anisotropy effects in $(L\omega)v/c^2$ via a reenactment of the Sagnac experiment using fiber optic gyroscopes (FOG) where L is the length of the fiber and ω is the angular speed of the FOG. We show how the fiber optics gyroscopes are used for constraining light speed anisotropy in the framework of the Mansouri-Sexl test theory. We also show an interesting amplification effect due to the use of the Mansouri-Sexl slow clock transport equations in conjunction with FOGs. Our paper is divided into four main sections: in the first one we give an overview of the Mansouri-Sexl test theory of special relativity, in the second one we give a historical perspective of the Sagnac experiment, in the third section we formulate the Mansouri-Sexl theory for the Sagnac experiment and we conclude with experimental setup and results.

Keywords: Mansouri-sexl test theory; light speed anisotropy; fiber optic gyroscopes.

[*]*Corresponding author: Email: egas@pacbell.net;*

1. INTRODUCTION - THE MANSOURI - SEXL TEST THEORY

The test theories [1-4] of special relativity are used to examine potential alternate theories to special relativity (SR) - such alternate theories predict particular values of the parameters of the test theory, which may easily be compared to values determined by experiments. The existing experiments put rather strong constraints on any alternative theory. One of these theories, the Robertson-Mansouri-Sexl theory, starts by admitting that there is one preferential inertial frame Σ in which the light propagates isotropically. In such a frame, light speed in a refractive medium is $c_0 = c/n$ where c is the light speed in vacuum and n is the refraction index of the optic fiber. All other frames in motion with respect to Σ are considered non-preferential and the light speed is anisotropic. The light speed in the non-preferential frames can be deduced via simple calculations described in[3]. We start with the Mansouri-Sexl transforms (with c=1):

$$\begin{aligned} \mathbf{x} &= d(v)\mathbf{X} + \frac{b(v)-d(v)}{v^2}\mathbf{v}(\mathbf{vx}) - b(v)\mathbf{v}T \\ t &= a(v)T + \boldsymbol{\varepsilon}(v)\mathbf{x} \end{aligned} \tag{1.1}$$

where **v** is the relative velocity between S and Σ, (x,t) are the coordinates in S while (X,T) represent their correspondents in Σ. Exactly like in the original Mansouri-Sexl paper [4] by transforming the light cone $X^2 - c_0^2 T^2 = 0$ into S and by neglecting the terms in v^2 and higher we obtain [2]:

$$\frac{c_{\pm}(\theta)}{c_0} \approx 1 \mp \frac{v}{c_0}(1+2\alpha)\cos\theta \tag{1.2}$$

where θ is the angle between the light ray direction and the x axis. Expression (1.2) is an approximation valid if slow clock transport [2-4] synchronization has been used. In this case, the following expressions also hold [2]:

$$\begin{aligned} a(v) &\approx 1 + \alpha(v)\frac{v^2}{c^2} \\ b(v) &\approx d(v) \approx 1 \\ \varepsilon &\approx 2\alpha v \end{aligned} \tag{1.3}$$

According to Mansouri and Sexl, the one-way light speed is a measurable quantity in this case and it is direction dependent for $\alpha \neq -0.5$. The larger the term $1+2\alpha$ in (1.2), the larger the light speed anisotropy. We will exploit this property in the Mansouri-Sexl theory of the FOG experiment constructed later in our paper.

On the other hand, according to Mansouri and Sexl [2], if Einstein clock synchronization is used, no first order effects exist and the second order effects are expressed as:

$$c(\theta) \approx \frac{c_0}{1+(\beta-\delta-1/2)(\frac{v}{c_0})^2 \sin^2\theta+(\alpha-\beta+1)(\frac{v}{c_0})^2} \tag{1.4}$$

where β,δ are parameters originating from the Taylor expansion of b,d respectively. In this case, the Sagnac effect cannot be used for measuring light speed anisotropy because the second order effects are too small to measure for any reasonable value for the speed v.

1.1. THE SPECIAL RELATIVITY THEORY OF THE SAGNAC EXPERIMENT USING FOG

A fiber optic gyroscope (FOG) senses changes in orientation, thus performing the function of a mechanical gyroscope. However its principle of operation is instead based on the interference of light which has passed through a coil of optical fiber. Two beams from a laser are injected into the same fiber but in opposite directions. Due to the Sagnac effect, the beam travelling against the rotation experiences a slightly shorter path delay than the other beam. The resulting differential phase shift is measured through interferometry, thus translating one component of the angular velocity into a shift of the interference pattern which is measured.

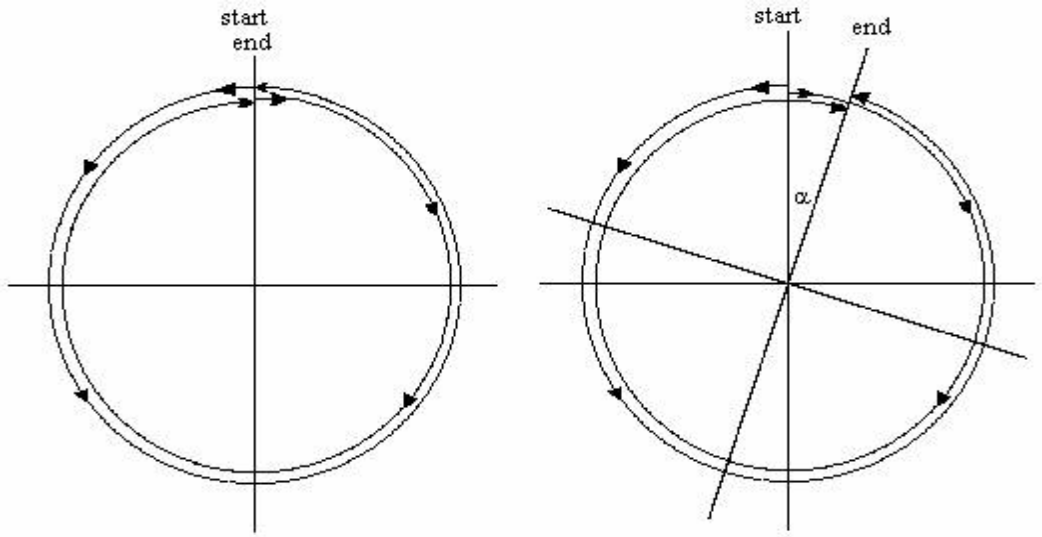

Fig. 1. Explanation of the sagnac experiment

The right hand side of Fig. 1 illustrates what happens if the loop itself is rotating. The symbol α denotes the angular displacement of the loop during the time required for the pulses to travel once around the loop. For any positive value of α, the pulse traveling in the same direction as the rotation of the loop must travel a slightly greater distance than the pulse traveling in the opposite direction. As a result, the counter-rotating pulse arrives at the "end" point slightly earlier than the co-rotating pulse. Quantitatively, if we let ω denote the angular speed of the loop, then the circumferential tangent speed of the end point is ωR. The respective angles traveled by the two light fronts are:

$$\phi_+ = 2\pi + \alpha_+ = \frac{c_+ t_+}{R} \tag{2.1}$$

for the co-rotating front

$$\phi_- = 2\pi - \alpha_- = \frac{c_- t_-}{R} \tag{2.2}$$

for the counter-rotating front,
where $c_+ = c_- = c$ in vacuum and:

$$\alpha_+ = \omega t_+ \tag{2.3}$$

for the co-rotating front

$$\alpha_- = \omega t_- \tag{2.4}$$

for the counter-rotating front.
Substituting (2.3) in (2.1) and (2.4) in (2.2) we get:

$$t_+ = \frac{2\pi R}{c - \omega R} \tag{2.5}$$

for the co-rotating front

$$t_- = \frac{2\pi R}{c + \omega R} \tag{2.6}$$

for the counter-rotating front. From (2.5) and (2.6) it follows that:

$$\Delta T_{total} = t_+ - t_- = \frac{4\pi R^2 \omega}{c^2 - R^2\omega^2} = \frac{4A\omega}{c^2 - R^2\omega^2} \tag{2.7}$$

where A is the area of the interferometer loop. The above is the exact formula. For $R\omega << c$ we recover the formula used in practice for detecting angular speed via the Sagnac experiment [5,6]:

$$\Delta T_{total} = \frac{4A\omega}{c^2} \tag{2.8}$$

The formula shows that the phase difference between the two counter-propagating light signals is, at low angular speeds, proportional to the angular speed and to the area enclosed by the interferometer loop. The first to perform a ring interferometer experiment aimed at observing the correlation of angular velocity and phase-shift was G. Sagnac [6] in 1913 with

the purpose of detecting "the effect of the relative motion of the ether". In 1926 a very ambitious ring interferometry experiment was set up by A. Michelson and H.Gale [7]. The aim was to find out whether the rotation of the Earth has an effect on the propagation of light in the vicinity of the Earth. The Michelson-Gale experiment used a very large ring interferometer, with a perimeter of 1.9 kilometer, so it was large enough to detect the angular velocity of the Earth. The outcome of the experiment was that the angular velocity of the Earth as measured by astronomical methods was confirmed to within measuring accuracy. The situation is a little more complicated in the case of using a fiber optic of refraction index n:

$$c_+ = \frac{\frac{c}{n} + \omega R}{1 + \frac{\omega R}{nc}}$$
$$c_- = \frac{\frac{c}{n} - \omega R}{1 - \frac{\omega R}{nc}} \tag{2.9}$$

Substituting (2.9) into (2.5)-(2.6):

$$t_+ = \frac{2\pi R}{c_+ - \omega R} = 2\pi R \frac{1 + \frac{\omega R}{nc}}{\frac{c}{n} - \frac{(\omega R)^2}{nc}} \tag{2.10}$$

for the co-rotating front

$$t_- = \frac{2\pi R}{c_- + \omega R} = 2\pi R \frac{1 - \frac{\omega R}{nc}}{\frac{c}{n} - \frac{(\omega R)^2}{nc}} \tag{2.11}$$

for the counter-rotating front, resulting into a total time:

$$\Delta T_{total\_SR} = t_+ - t_- = \frac{4\pi R^2 \omega}{c^2 - R^2\omega^2} \tag{2.12}$$

Interestingly enough, the outcome of the experiment does not depend on the refraction index of the fiber optic. The SR prediction from expression (2.12) fully coincides with the experimental results [9]. One of the important advantages of FOGs, besides the absence of any moving parts is the fact that the optic cables can be wrapped around k times resulting into an “amplification” of the net effect:

$$\Delta T_{total\_SR} = k\frac{4\pi R^2\omega}{c^2 - R^2\omega^2} \tag{2.13}$$

The resulting phase difference is:

$$\Delta S_{total\_SR} = c\Delta T_{total\_SR} = kc\frac{4\pi R^2\omega}{c^2 - R^2\omega^2} \approx \frac{4\pi R^2 k\omega}{c} \tag{2.14}$$

that is, the effect is the first order in $\frac{\omega}{c}$, "amplified" by the length of the fiber, $L = 2\pi Rk$ and by the radius of the gyroscope, R.

2. THE MANSOURI-SEXL THEORY OF THE FOG EXPERIMENT

Light speed is propagating with the isotropic speed c_0 in the preferential frame. In the non preferential frame S associated with the center of the rotating FOG device light speed propagates at the speeds c_+ in the direction of rotation and c_- in the direction against the rotation of the device (Fig. 2).

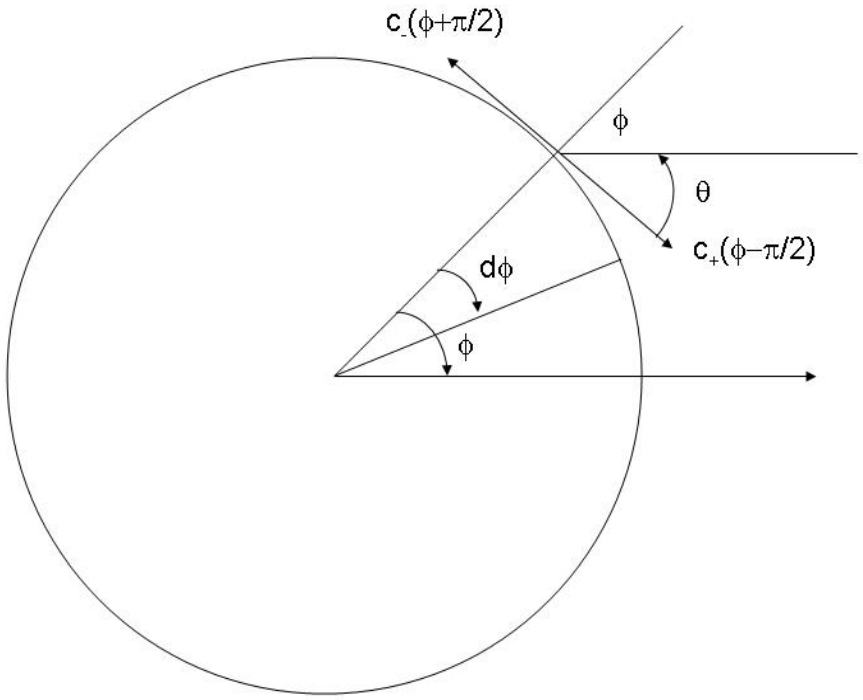

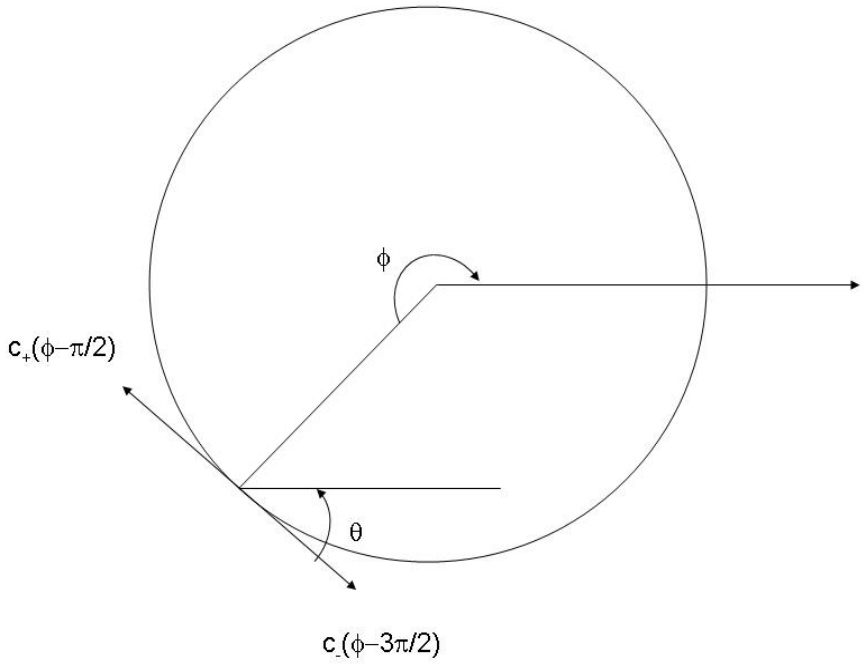

Fig. 2. Detail of the experiment with anisotropic light speed

where, for an infinitesimal angle of rotation $d\phi$:

$$c_+\Delta t_+ = Rd\phi + \omega R\Delta t_+ \tag{3.1}$$

for the co-rotating front

$$c_-\Delta t_- + \omega R\Delta t_- = Rd\phi \tag{3.2}$$

for the counter-rotating front.

$$\Delta t_+ = \frac{Rd\phi}{c_+ - \omega R} \tag{3.3}$$

for the co-rotating front

$$\Delta t_- = \frac{Rd\phi}{c_- + \omega R} \tag{3.4}$$

for the counter-rotating front. From (3.3) and (3.4) it follows that the phase difference element is:

$$\Delta s = c_+ \Delta t_+ - c_- \Delta t_- = R^2 \omega d\phi \frac{(c_- + c_+)}{(c_- + \omega R)(c_+ - \omega R)} \tag{3.5}$$

Formula (3.5) is a generalization of formula (21) in reference [8]. On the other hand, according to Fig. 2, light speed appears to be anisotropic in frame S, associated with the center of the rotating FOG, such that for slow clock transport synchronization and for $\phi \in [0, \pi]$ the following holds by (1.2):

$$\frac{c_+}{c_0} \approx 1 - \frac{v}{c_0}(1+2\alpha)\cos(\phi - \frac{\pi}{2}) = 1 - \frac{v}{c_0}(1+2\alpha)\sin\phi \tag{3.6}$$

for the co-rotating front

$$\frac{c_-}{c_0} \approx 1 - \frac{v}{c_0}(1+2\alpha)\cos(\phi + \frac{\pi}{2}) = 1 + \frac{v}{c_0}(1+2\alpha)\sin\phi \tag{3.7}$$

for the counter-rotating front.

For $\phi \in [\pi, 2\pi]$ c_+ and c_- exchange roles. Substituting (3.6) and (3.7) into (3.5) we obtain:

$$\Delta s \approx \frac{2R^2 \omega c_0 d\phi}{{c_0}^2 - [v(1+2\alpha)\sin\phi + \omega R]^2} \tag{3.8}$$

The total phase differential between the two light paths obtained through the integration of the phase difference element is:

$$\Delta S_{total\_MS}(v, \alpha, \omega) \approx 4R^2 \omega c_0 k \int_0^{\pi} \frac{d\phi}{{c_0}^2 - [v(1+2\alpha)\sin\phi + \omega R]^2} \tag{3.9}$$

The doubling of the integral (3.9) is caused by c_+ and c_- exchanging roles in the interval $\phi \in [\pi, 2\pi]$. Using the notation $A(v, \alpha) = v(1+2\alpha)$ (A is a function of v and α) and $B = \omega R$ we obtain:

$$\Delta S_{total\_MS} \approx 2\pi R^2 \omega k \left(\frac{1}{\sqrt{(B - c_0)^2 - A^2}} + \frac{1}{\sqrt{(B + c_0)^2 - A^2}}\right) \tag{3.10}$$

A quick sanity check shows that in SR $\alpha = -0.5$ (i.e. $A = 0$ in (3.10)) so we recover the well known SR expression (2.7):

$$\Delta S_{total\_SR} = \frac{4\pi R^2 \omega k c_0}{{c_0}^2 - (\omega R)^2} \tag{3.11}$$

That is, in SR the phase difference is independent of the speed between the lab and the "preferential" frame Σ. Given that $v \ll c_0$, the effect is very close to null for non-rotating devices. The difference:

$$\Delta S_{violation} = \Delta S_{total\_MS} - \Delta S_{total\_SR} \tag{3.12}$$

is the actual Mansouri-Sexl violation expressed in terms of fraction of a fringe (in μm) and it is a function of the Mansouri-Sexl parameter α, the angular speed ω of the FOG with respect to the lab frame S and the relative speed of the lab v with respect to the preferential frame Σ. As it can be seen from (3.9), any deviation from -0.5 for the parameter α attracts a dependency of the result in terms of the speed v between S and Σ. As opposed to the case of the SR formula (2.12), the Mansouri-Sexl formula (3.10) depends on the refraction index via $c_0 = c/n$ restricting the constraining of the parameter α to experiments that must use fiber optics with refraction indexes close to unity. The difference is due to the fact that formulas (3.6) and (3.7) are just approximations in the Mansouri-Sexl theory whereas formula (2.9) is exact. In our experiment, we made use of the above prediction in order to set constrains on light speed anisotropy.

The laboratory velocity $v(t)$ has contributions [10-19] from the motion of the Sun with respect to frame Σ with a constant velocity $v_s = 377 km/s$, while Earth's orbital motion around the Sun $v_e = 30 km/s$. For example, in the case of the references [10-19] the Earth's daily rotation speed is $v_d = 0.33 km/s$ while for Berkeley, where the experiment was executed (latitude 37°52'18" N) $v_d = 0.355 km/s$. Finally, $v_r = \omega R$ is the active rotation speed of the FOG so:

$$v(t) = v_s + v_e \sin[\Omega_y (t - t_0)] \cos\Phi_E + v_d \sin[\Omega_d (t + t_d)] \cos\Phi_A + v_r \sin(\omega t) \cos\Phi_B \tag{3.13}$$

Here $\Phi_A \approx 8^o$ is the angle between the equatorial plane and the velocity of the sun. $\Phi_E \approx 6^o$ is the declination between the plane of Earth's orbit and the velocity of the Sun, $\Phi_B \approx 33^o$ is the declination between the plane of FOG plane and the velocity of the Sun, $2\pi / \Omega_y = 1 yr$, $2\pi / \Omega_d = 1$ sidereal day, t_0 and t_d are determined by the phase and start date of the measurement, respectively. If $\alpha \neq -0.5$ then the sinusoidal time variation of v will be reflected in the phase difference (3.10). In other words, the phase difference (3.10) will exhibit a characteristic time signature when measured over a sufficiently long time. In order to constrain the parameter α we will take a series of measurements at different angular speeds ω over periods of time long enough such that we could integrate the sinusoidal effects shown in (3.13). From expression (3.13) we can see that $v(t) << c_0$. This enables us to further simplify expression (3.10) and, subsequently, (3.12) by using Taylor expansion such that we can express the translational effects in v in a simpler form:

$$\Delta S_{total\_MS} \approx \frac{4\pi R^2 k\omega}{c_0} + 4\pi R^2 k\omega(1+2\alpha)\frac{v}{c_0^2} = \frac{(4\pi R^2 kn)\omega}{c} + 2Rn^2(1+2\alpha)\frac{(2\pi Rk\omega)v}{c^2} \quad (3.14)$$

The amplification of the effect due to the presence of large values of the coil number k is a game changer since we can achieve $2\pi Rk\omega >> v$ for suitable optical cable lengths even with moderate angular speeds of rotating the FOG. In his analysis, made 14 years ago, Stedman [5] expressed pessimism that FOGs can be used in the detection of light speed anisotropy but FOGs have made huge advancements in the past decade, not only in terms of precision but also in terms of the fiber optic length. For example, in our experimental setup, $2\pi Rk\omega = 1200m$. In order to constrain the parameter α we will take a series of measurements at different angular speeds ω over periods of time long enough such that we could integrate the sinusoidal effects shown in (3.13). Substituting (3.13) into (3.14) we obtain:

$$\Delta S_{total\_MS} = C_0 + C_{11}\sin(\Omega_y t) + C_{12}\cos(\Omega_y t) + C_{21}\sin(\Omega_d t) + C_{22}\cos(\Omega_d t) + C_3\sin(\omega t) \quad (3.15)$$

where

C_0	$\frac{4\pi R^2 k\omega n}{c} + \frac{4\pi R^2 k\omega n^2}{c}(1+2\alpha)\frac{v_s}{c}$
C_{11}	$\frac{4\pi R^2 k\omega n^2}{c}(1+2\alpha)\frac{v_e}{c}\cos(\Omega_y t_0)\cos\Phi_E$
C_{12}	$-\frac{4\pi R^2 k\omega n^2}{c}(1+2\alpha)\frac{v_e}{c}\sin(\Omega_y t_0)\cos\Phi_E$
C_{21}	$\frac{4\pi R^2 k\omega n^2}{c}(1+2\alpha)\frac{v_d}{c}\cos(\Omega_d t_d)\cos\Phi_A$
C_{22}	$\frac{4\pi R^2 k\omega n^2}{c}(1+2\alpha)\frac{v_d}{c}\sin(\Omega_d t_d)\cos\Phi_A$
C_3	$\frac{4\pi R^2 k\omega n^2}{c}(1+2\alpha)\frac{\omega R}{c}\cos\Phi_B$

(3.16)

For $\alpha = -0.5$ we recover the SR prediction $\Delta S_{total\_MS} = \Delta S_{total\_SR} = \frac{4\pi R^2 k\omega n}{c}$. The second observation is that the coefficient C_0 is much larger than the other coefficients in the Fourier expansion.

3. THE EXPERIMENTAL SETUP AND THE RESULTS

We used two experimental setups, both based on commercially available FOGs. One uses EMP-1.2k, ($1.2\text{km coil}, n = 1.1$) and the other one uses EMP-1 ($200\text{m coil}, n = 1.1$), both from Emcore Inc mounted on a Yaskawa SGMJV Sigma-5 high precision turntable with variable angular speed (Fig. 3). We made four sets of measurements, alternating between the two FOGs, in a 24 hr interval, at 6 hours intervals in order to best capture the effects of the variation of the Earth speed expressed in (3.14) as well as the diurnal changes of temperature affecting the FOGs. Each set of measurements is composed of 10 runs, labeled

0-9. We repeated the measurements sets four times, at different angular speeds, varying from $\omega = 30$ to $\omega = 150$. The $\Delta S_{violation}$ measurements, expressed in μm, including the calculation of the error bars, are presented in Tables 1 through 4.

Table 1. $\Delta S_{violation}$ measurements at 6 am

ω=30	1	2	3	4	5	6	7	8
Series1	0.4186667	0.418667	0.4186667	0.4186667	0.41866693	0.41866676	0.4186666	0.41985027
Series2	0.4186668	0.418665	0.4186667	0.4186667	0.41866671	0.418666667	0.4186666	0.41985067
Series3	0.4186666	0.418667	0.41866672	0.4186733	0.41866672	0.418666677	0.4186667	0.41985036
Series4	0.4186668	0.418666	0.41866668	0.4186667	0.41866673	0.418666668	0.4186666	0.41985304
STD DEV	7.414E-08	5.27E-07	2.1344E-08	3.313E-06	1.0722E-07	4.49526E-08	3.2E-08	1.3136E-06
STD ERR	1.853E-08	1.32E-07	5.3359E-09	8.283E-07	2.6805E-08	1.12382E-08	8.001E-09	3.284E-07

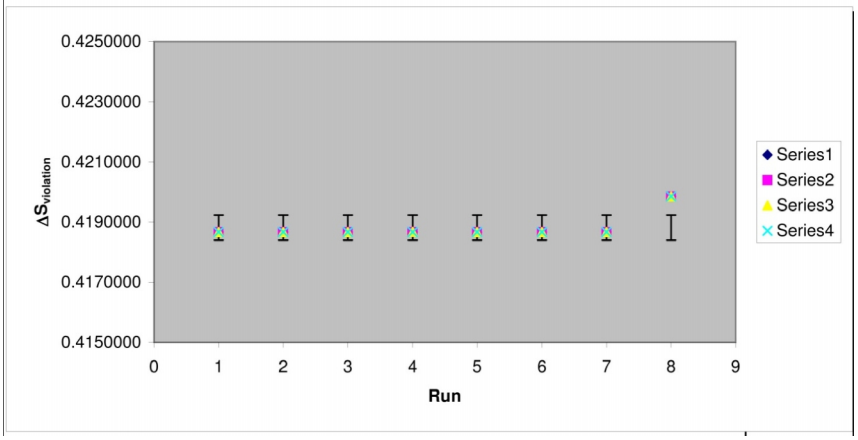

Table 2. $\Delta S_{violation}$ measurements at 12 pm

ω=50	1	2	3	4	5	6	7	8
Series1	0.6977778	0.697778	0.6977778	0.6977778	0.69777822	0.697777933	0.6977777	0.69775282
Series2	0.6977780	0.697776	0.6977778	0.6977779	0.69777784	0.697777778	0.6977777	0.69775289
Series3	0.6977777	0.697778	0.69777787	0.6977789	0.69777787	0.697777796	0.6977778	0.69775284
Series4	0.6977780	0.697777	0.6977778	0.6977779	0.69777789	0.697777779	0.6977777	0.69775306
STD DEV	1.236E-07	8.79E-07	3.5573E-08	5.232E-07	1.787E-07	7.4921E-08	5.334E-08	1.0972E-07
STD ERR	3.089E-08	2.2E-07	8.8932E-09	1.308E-07	4.4675E-08	1.87303E-08	1.333E-08	2.7431E-08

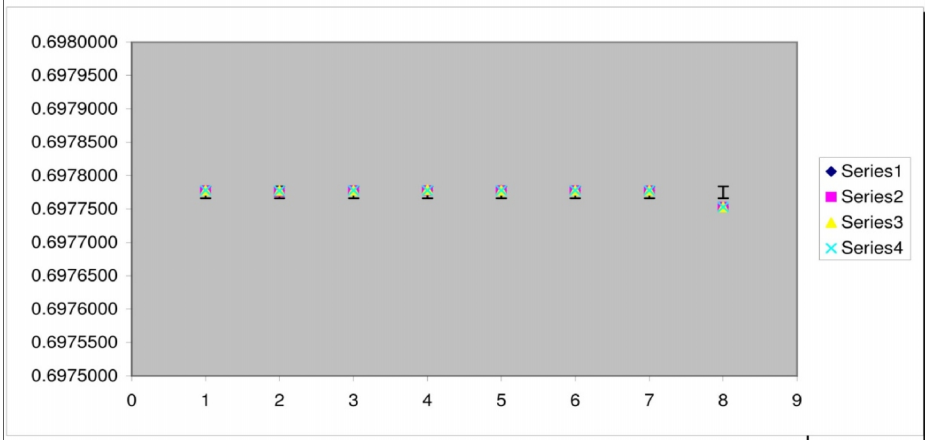

Table 3. $\Delta S_{violation}$ measurements at 6 pm

ω=100	1	2	3	4	5	6	7	8
Series1	1.3955556	1.395555	1.3955556	1.3955556	1.39555644	1.395555867	1.3955553	1.39550564
Series2	1.3955559	1.395552	1.3955556	1.3955557	1.39555569	1.395555556	1.3955553	1.39550573
Series3	1.3955555	1.395555	1.39555573	1.3955578	1.39555573	1.395555591	1.3955556	1.39550568
Series4	1.3955560	1.395554	1.3955556	1.3955557	1.39555578	1.395555559	1.3955555	1.39550572
STD DEV	2.471E-07	1.76E-06	7.1146E-08	1.046E-06	3.574E-07	1.49842E-07	1.067E-07	4.1595E-08
STD ERR	6.178E-08	4.4E-07	1.7786E-08	2.616E-07	8.9351E-08	3.74605E-08	2.667E-08	1.0399E-08

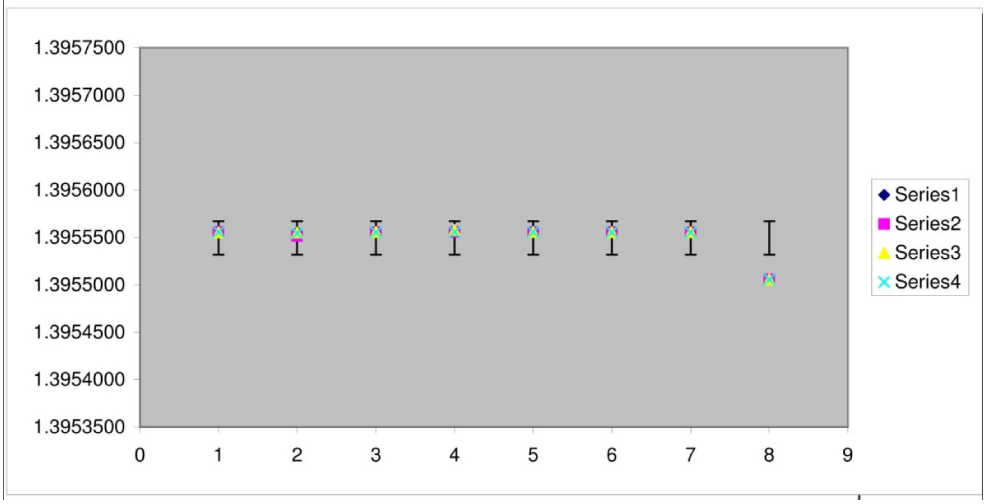

Table 4. $\Delta S_{violation}$ measurements at 12 am

ω=150	1	2	3	4	5	6	7	8
Series1	2.0933333	2.093333	2.0933334	2.0933334	2.09333467	2.0933338	2.0933330	2.09325913
Series2	2.0933339	2.093327	2.0933334	2.0933336	2.09333353	2.093333334	2.093333	2.09325927
Series3	2.0933332	2.093333	2.0933336	2.0933367	2.0933336	2.093333387	2.0933333	2.09325918
Series4	2.0933339	2.093331	2.0933334	2.0933336	2.09333367	2.093333338	2.0933332	2.0932600
STD DEV	3.707E-07	2.64E-06	1.067E-07	1.57E-06	5.361E-07	2.24763E-07	1.6E-07	4.0634E-07
STD ERR	9.267E-08	6.59E-07	2.668E-08	3.924E-07	1.3403E-07	5.61908E-08	4E-08	1.0158E-07

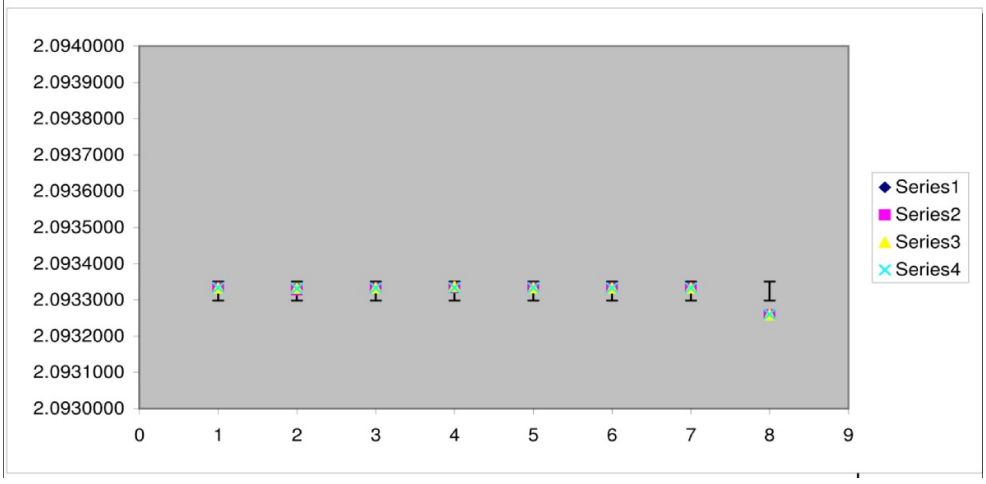

Based on the measurements we developed a best fit approximation in the form of a Fourier expansion:

$$\Delta\hat{S} = \hat{C}_0 + \hat{C}_{11}\sin(\Omega_y t) + \hat{C}_{12}\cos(\Omega_y t) + \hat{C}_{21}\sin(\Omega_d t) + \hat{C}_{22}\cos(\Omega_d t) + \hat{C}_3\sin(\omega t) \quad (4.1)$$

The standard error in the determination of $\hat{C}_0$ is equal to 1.33×10^{-14}. Comparing with (3.16) and taking into considerations the characteristics of the FOGs employed, this results into a constraint of $|\alpha+0.5|<(1.2\pm0.83)\times10^{-6}$ for the parameter α.

Fig. 3. The experimental setup

The measurement errors can be attributed in totality to the systematic errors introduced by the FOG devices and the turntable, better results will be obtained in the next generation of the experiments when more precise FOGs become available and we can get a better control over maintaining constant angular speed of the underlying turntable.

3.1. FUTURE WORK AND COMPARISON WITH OTHER METHODS

Presently, the method using FOGs results into lesser constraints than the methods using resonating cavities [10-19]. On the other hand, our results are better by an order of magnitude than the ones of Champeney et al. [20] while being one order of magnitude less restrictive than the experiment executed by Isaak [21]. We plan to repeat the measurements as higher precision FOGs become available. The nice aspect about using FOGs is that they have no moving parts and that their technology is advancing very quickly, both reasons for increasing precision over time. Thus, we can put ever tightening constraints over the Mansouri-Sexl parameter α using commercially available equipment that costs a fraction of the price of the specially designed equipment for such kind of experiments.

4. CONCLUSION

We have developed the Mansouri-Sexl theory for the FOG experiment. We have shown that the Mansouri-Sexl violation is a function of the Mansouri-Sexl parameter α, the angular speed ω and of the relative speed of the lab v with respect to the preferential frame Σ. We have shown how the FOG experiment can be used in order to detect light speed anisotropy

within the framework of the Mansouri-Sexl theory and we constrained the parameter α to less than $-0.5\pm0.83\times10^{-6}$.

AKNOWLEDGEMENTS

The author is grateful for the suggestions of the anonymous referees. The research in this paper was self-funded.

COMPETING INTERESTS

Author has declared that no competing interests exist.

REFERENCES

1. Robertson HP. Postulate versus Observation in the Special Theory of. Relativity, Rev. of Mod. Phys. 1949;21:378-382.
2. Mansouri R, Sexl SU. A test theory of special relativity: I. Simultaneity and Clock Synchronization, Gen. Rel. Grav. 1977;8:497-513.
3. Mansouri R, Sexl SU. A test theory of special relativity: II. First Order Tests, Gen. Rel. Grav. 1977;8;515-524.
4. Mansouri R, Sexl SU. A test theory of special relativity: III. Second Order Tests,Gen. Rel. Grav. 1977;8:809-814.
5. Stedman GE. Ring-laser tests of fundamental physics and geophysics, Rep. Prog. Phys. 1997;60:615-688.
6. Sagnac G. L'Ether lumineux demontre par l'effet du vent relatif d'ether dans un interferometre en rotation uniforme, Comptes Rendus de l'Academie des Sciences (Paris). 1913;157:708-710,1410-1413.
7. Michelson A, Gale H, Pearson F. The Effect of the Earth's Rotation on the Velocity of Light (Parts I and II), Astrophysical Journal. 1925;61:137-145.
8. Rizzi G, Ruggiero ML. Relativistic Physics in Rotating Reference Frames, Kluwer Academic Publishers-Netherlands; 2004.
9. Wang R, Zheng Y, Yao A, Langley D. Modified Sagnac experiment for measuring travel-time difference between counter-propagating light beams in a uniformly moving fiber, Phys.Lett. A. 2003;312:7-10.
10. Saathoff G, Karpuk S, Eisenbarth U, Huber G, Krohn S, Horta RM, et al. Improved test of time dilation in special relativity, Phys. Rev. Lett. 2003;91(19):190403.
11. Müller H, Herrmann S, Braxmaier C, Schiller S, Peters A. Modern Michelson-Morley experiment using cryogenic optical resonators, Phys. Rev. Lett. 2003;91:020401.
12. Müller H, Herrmann S, Braxmaier C, Schiller S, Peters A. Theory and technology for a modern Michelson-Morley Test of Special Relativity, Appl. Phys. B; 2003.
13. Müller H, Braxmaier C, Herrmann S, Pradl O, Lämmerzahl C, Mlynek J, et al. Testing the foundations of relativity using cryogenic optical resonators, Int. J. Mod. Phys. D. 2002;11.
14. Müller H, Braxmaier C, Herrmann S, Peters A, Lämmerzahl C. Electromagnetic cavities and Lorentz invariance violation, Phys. Rev. D 67, 056006; 2003.
15. Lipa JA. New Limit on Signals of Lorentz Violation in Electrodynamics, Phys. Rev. Lett. 90 060403; 2003.
16. Braxmaier C, Müller H, Pradl O, Mlynek J, Peters A, Schiller S. Test of Relativity using a cryogenic optical resonator, Phys. Rev. Lett. 2002;88.

17. Schiller S, Antonini P, Okhapkin M. A precision test of the isotropy of the speed of light using rotating cryogenic optical cavities, Phys. Rev. Lett. 2005;95.
18. Wolf P, Bize S, Clairon A, Santarelli G, Tobar ME, Luiten AN. Improved Test of Lorentz Invariance in Electrodynamics, Phys. Rev. 2004;D(70).
19. Ahmed F, Quine BM, Sargoytchev S, Stauffer AD. A Review of Speed of Light, IJP, accepted; 2011.
20. Champeney DC, Isaak GR, Khan AM. An 'aether drift' experiment based on the Mössbauer effect, Phys. Lett. 1963;7(4):241-243.
21. Isaak GR. The Mossbauer effect: Application to relativity, Phys. Bull. 1970;21:255.

Peer-review history:
The peer review history for this paper can be accessed here:
http://www.sciencedomain.org/review-history.php?iid=216&id=4&aid=1193